CHARACTERIZATION OF THE ELECTRON BEAM CURE PROCESS OF AN

EPOXY - INITIATOR SYSTEM

A Thesis

by

RAHUL RIBEIRO

Submitted to the Office of Graduate Studies of
Texas A&M University
in partial fulfillment of the requirements for the degree of

MASTER OF SCIENCE

May 2003

Major Subject: Mechanical Engineering

CHARACTERIZATION OF THE ELECTRON BEAM CURE PROCESS OF AN
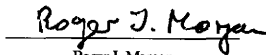
EPOXY - INITIATOR SYSTEM
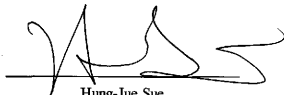
A Thesis

by

RAHUL RIBEIRO

Submitted to Texas A&M University
in partial fulfillment of the requirements for the degree of

MASTER OF SCIENCE
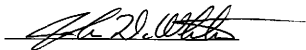
Approved as to style and content by:

_____
Roger J. Morgan
(Chair of committee)

_____
Hung-Jue Sue
(Member)

_____
John D. Whitcomb
(Member)

_____
John Weese
(Head of Department)

May 2003

Major Subject: Mechanical Engineering

ABSTRACT

Characterization of the Electron Beam Cure Process of an Epoxy – Initiator System.

(May 2003)

Rahul Ribeiro, B.S., Marine Engineering and Research Institute, India

Chair of Advisory Committee: Dr. Roger J. Morgan

For over forty years high energy electrons have been used to change polymer structure and properties. In this thesis we study the potential use of a high energy electron beam (e-beam) to replace the thermal curing method and offset some of it's disadvantages which are: inability to cure large parts, release of harmful volatiles and high manufacturing and tooling costs. Electron beam curing of the Diglycidyl Ether of Bisphenol A (DGEBA) – $I^+SbF_6^-$ resin initiator system was studied with emphasis on the cure rate, initiator concentration, degree of cure and glass transition temperature. Basic models based on previous thermal curing studies are developed to determine the material properties during cure. It was found that the maximum glass transition temperature obtained was below 100 °C for all initiator concentrations used. The cure rate followed typical arrhenius curves for autocatalytic curing behavior, similar to thermal curing. The cure rate increased with increase in initiator concentration. The temperature profile measured in – situ, and the effects of impurities present were also investigated. Finally the models developed indicate the potential to model and program the cure process to develop materials with desired properties.

ACKNOWLEDGMENTS

Firstly, I wish to thank Lord Jesus and my parents for supporting me and providing me with an interesting life which has been spent on four continents so far. Next, I wish to thank my advisor Dr. Roger J. Morgan, who sincerely supported and guided me through my graduate studies. I also wish to thank my other committee members, Dr. Hung-Jue Sue and Dr. John D. Whitcomb, for their support and guidance. A special 'thank you' to Dr. Terry Creasy for kindly obliging to substitute on my committee in the absence of Dr. Hung-Jue Sue. I thank the Air Force Office of Scientific Research sponsored by Dr. Charles Lee and the Advanced Project Research program of the State of Texas for financial support and encouragement of this study. Last but not the least, I wish to thank my colleague, Dr. Sung-Won Moon, for his help and co-operation that helped me immensely in successfully completing this thesis.

TABLE OF CONTENTS

LIST OF FIGURES

CHAPTER I

INTRODUCTION

In the area of high-performance polymers, there is a never-ending desire for materials with improved thermal and dimensional stability, a higher modulus, greater tensile strength, a lower coefficient of thermal expansion, and a lighter mass. Thermosets are found to provide certain advantages over other materials some of which are: excellent chemical and corrosion resistance, excellent thermal properties and low creep, high stiffness and modulus properties, easy to process in low cost equipment, high strength to weight ratios and resistance to flame spread. Some of their disadvantages include moisture absorption, toxicity and they are non recyclable.

A thermoset is defined as a polymeric material which can be formed by the application of heat and pressure, but as a result of a chemical reaction, permanently crosslinks and cannot be reformed upon further application of heat and pressure. The phenomenon of 'crosslinking' (refer to Figure 1) is known as 'curing'. Thermosetting resins are often liquid at some stage in their manufacture or processing, which are cured by heat, radiation, catalysis or other chemical means. After being fully cured, thermosets cannot be resoftened by heat. Some plastics which are normally thermoplastic can be made thermosets by means of crosslinking with other materials. The word 'thermo' implies that the crosslinking proceeds through the influence of heat energy input and the term 'setting' references the fact that an irreversible reaction has occurred on a macro scale [1].

Thermosetting polymers are formed by: polymerizing monomers where at least one of them has a functionality higher than two and by chemically creating crosslinks between previously formed linear or branched macromolecules. In fully reacted polymer networks, practically all constituent units are covalently bonded into an infinite three-dimensional structure. It means that during polymerization or

This thesis follows the style of *Journal of Composite Materials*.

crosslinking, the system evolves from a collection of molecules of finite size to an infinite network, proceeding through the gel point at which the infinite network structure appears for the first time. This transformation is called 'gelation' [2].

Gelation is characteristic of thermosets, and it is of great significance. From a processing standpoint, gelation is critical since the polymer will not flow, and is no

E is a tetra-functional Epoxy monomer
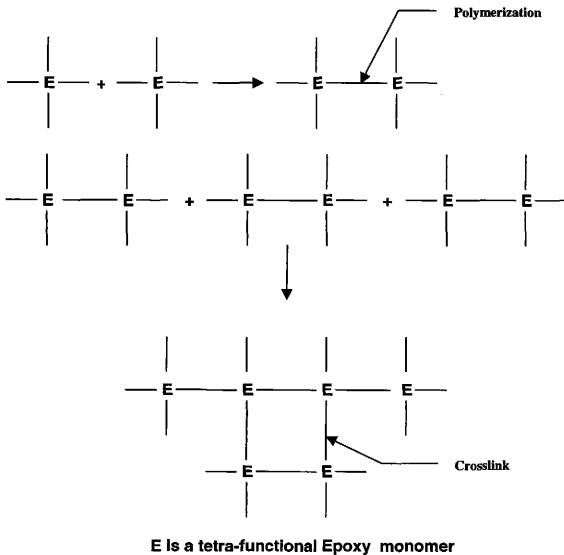
Figure 1. Polymerization and crosslinking of an epoxy

longer processible beyond this point. "Gelation occurs at a well defined and calculable stage during the chemical reaction and is dependent on the functionality, reactivity, and stoichiometry of the reactants" [3]. Gelation typically occurs between 45 and 80% conversion (degree of cure, defined as the number of species reacted, divided by the total number of species available for reaction initially, $\alpha = 0.45$ to 0.8). "Means to detect gelation include the abrupt inability of bubbles to rise in the thermosetting mass and the rapid approach to infinite viscosity. Gelation does not, however, inhibit the curing process and cannot be detected by techniques sensitive only to the chemical reaction" [4]. Beyond the gel point, the reactions proceed towards the formation of an infinite network with substantial increase in crosslink density, glass transition temperature and ultimate physical properties.

Another phenomenon that may occur at a certain stage during cure is the 'vitrification' of the growing chains or network [4]. Vitrification is the process of transformation of the resin from a viscous liquid or elastic gel to a glass. This process begins to occur as the glass transition temperature of these growing chains or network becomes coincidental with the cure temperature. Further curing in the glassy state is extremely slow and, in practice, vitrification brings an abrupt halt to curing. Vitrification is a reversible transition and cure may be resumed by heating to 'devitrify' the partially cured thermoset [5].

Influence of Time, Temperature, Mass and Initiator

The temperature dependency of crosslinking reactions has almost always been found to behave in a traditional Arrhenius relationship. For example the Equation would be in the form:

$$Rate\ of\ cure = -A\exp(\frac{-E_a}{R.T})f(x) \tag{1}$$

Where:

      A is the temperature independent collision factor

      E_a is the activation energy for a single reaction

R is the universal gas constant

T is the absolute temperature

$f(x)$ is a function of the number of reactive species x

Thus temperature strongly influences the crosslinking rate. Since all commercial thermosetting reactions are exothermic, the amount of mass present also influences the rate of reaction due to the temperature increase. "Monomer concentration effects are generally associated with stoichiometric balances between reactants as well as the normal free volume accessibility of each of the reactants to each other" [1]. Referring to Figure 2, we can observe the viscosity change versus time at a given temperature. Beginning at time t_0, the viscosity is η_0. The heat generated due to the exothermic reactions produces a typical viscosity decrease η_1. As the molecular weight of the mass increases, the resultant viscosity increase outpaces and surpasses any reduction caused by heat. The molecular growth continues until the gel point is reached. At the gel point the viscosity increases to infinity and the material theoretically cannot flow. The effect of the initiator or catalyst is to speed up the reactions and has the tendency of either decreasing the activation energy E_a, or increasing the collision factor A. Therefore the percentage of initiator present will also have an effect on the molecular weight and hence on the properties of the material.

Composite

A thermoset is sometimes reinforced with polymeric fibers to form polymeric matrix fibrous composites (PMFCs). "A composite is a material comprised of two or more physically distinct materials with at least one material providing reinforcing properties on strength and modulus. The components of a composite do not dissolve or otherwise merge completely into each other, but nevertheless do act in concert. The properties of a composite cannot be achieved by any of the components acting alone. Composites can be classified on the basis of the form of their structural components: fibrous (composed of fibers in a matrix), layers (composed of layers of

materials), and particulate (composed of particles in a matrix). In general, the reinforcing agent can be either fibrous, powdered, spherical, crystalline, or whiskered and either an organic, inorganic, metallic or ceramic material" [6].
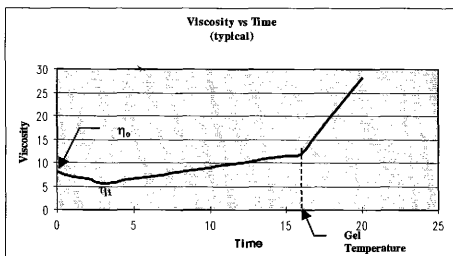
Figure 2. Change in viscosity with time during cure (typical)

Examples of resins being used [6]

- Unsaturated Polyester
- Vinyl Esters
- Polybutadiene
- Epoxies
- Polyimides (high temperature)
- Bismaleimides

Examples of fiber materials [6]

- Glass

- Paper (cellulosic fiber)
- Cotton
- Polyamides
- Asbestos
- Sisal
- Jute

Fibers used for high performance

- Carbon
- Kevlar
- Boron
- Steel
- Whiskers (a very short form of reinforcement, usually of crystalline material)

These fiber reinforcing agents are quite diverse with respect to cost, composition, and properties.

In this thesis we study the radiation cure process of an epoxy resin – initiator system. Epoxy resins are among the best matrix materials for many fiber composites. The reasons for this are:

- Epoxy resins adhere well to a wide variety of fillers, reinforcing agents, and substrates.
- A wide variety of available epoxy resins and curing agents can be formulated to give a broad range of properties after cure and to meet a diverse spectrum of processing requirements.
- Cured epoxy resins are resistant to chemicals and heat, provide good electrical insulation and have good mechanical strength.

Epoxy resins are used in various composites and in many structural parts. They are also used as potting and encapsulating compounds, tooling compounds, molding powders and adhesives [6].

In the aerospace industry polymer matrix fibrous composites (PMFCs) are used in various structural components due to their light weight, toughness and low cost. Other desirable properties are extremely low shrinkage, low void content, low moisture absorption and low vacuum outgassing as well as excellent mechanical properties over a wide range of temperatures [7].

Thermal Curing

In this method of curing, the energy required to activate the reactions is provided by heating the thermoset in an autoclave.

Advantages

- The reaction mechanisms are easy to study
- It is a well developed process
- Almost all resin-curing agent combinations as well as cationic can be cured.

Disadvantages

- There is a limit to the size of the component that can be cured
- High manufacturing and tooling costs
- The part has to be cured as a whole and there is no means of localized curing
- Toxic volatiles can be evolved

Radiation Curing

In this method of curing, the activation energy is provided by submitting the thermoset to high energy X-rays, γ–rays, or electron beams (e-beams). The E-beam cure process mechanism of composite resin thermosets involves high-energy electrons striking atoms and molecular bonds of the resin monomers resulting in the transfer of energy by the following mechanisms:

- Energy transfer to the electrons of the atoms of the resin target monomers. Such electrons may then be either expelled from the atoms, yielding positively charged ions and free electrons, or shifted to a higher-energy atomic orbital producing an excited atom or molecule. These ions, electrons and excited species are the precursors that initiate and propagate the resin cure reactions [8].

- Energy transfer to molecular bonds, such as carbon-hydrogen bonds, causing rupture of the bonds with release of hydrogen and the formation of excited carbon atom free radicals.

Advantages

- Ability to cure large parts
- Lower manufacturing costs
- Simplified processing
- Lower cure temperatures
- Environmentally friendly
- Localized curing possible
- Reduction of volatiles

Disadvantages

- The reaction kinetics are not properly understood
- The radiation is harmful to personnel
- The composites suffer from low compressive strength
- Have a poor interface between fiber and matrix
- Have low inter-laminar shear strength
- Have low fracture toughness

Composite Use in the Aerospace Industry

In the aerospace industry, the Air Force is developing a Space Operations Vehicle (SOV) which will have more stringent performance requirements than NASA's reusable launch vehicle, that will involve higher usage rates and G maneuvers, shorter turn around times and longer alert times [9].

These aeropropulsion technological developments require lightweight, tough, low cost structures of which the health and safety are well characterized. The use of new, high performance polymeric matrix fibrous composites (PMFCs) for the liquid hydrogen (LH$_2$) and liquid oxygen (LOX) containment structures will allow a critical lightweight, single stage to orbit (SSTO) launch vehicle. Such structures are cryogenic fuel tanks, feedlines, and struts and support structures. The utilization of lightweight, cryogenic tough PMFCs with also high temperature performance capabilities (-423 ^{o}F to 250 ^{o}F) will be critical in the development of these space vehicles. The SOV composite cryogenic tank technical 'whole life cycle' requirements are:

Cryogenic and high temperature composite performance in terms of:
- Long term cryogenic durability
- Thermal cycle-shock damage resistance
- Cryogenic fuel solubility and permeability in the PMFC
- Meaningful accelerated test procedures
- Materials that involve the development of:
  - Matrices that are tough over a wide temperature range, with low cryogenic fuel permeability
  - Non-autoclave fabrication of large composite structures
  - Innovative design procedures of composites for maximum microcrack resistance

Advanced composites, such as the load-bearing members in an aerospace structure, often attain maximum mechanical properties and unique physical

characteristics. This can be achieved by obtaining high fiber-to-resin ratio, using continuous fibers, and designing the fiber orientation.

The ability to monitor the local temperature rise in the composite is limited by thermocouple monitoring systems and it is believed that the local microscopic temperature rise maybe higher than that recorded macroscopically. Large differences in temperature within the material during cure can severely affect the thermo-mechanical properties. Also there is a difference in the rate of heat absorbed and temperature rise between the fiber and resin while curing a composite. The fiber tends to heat up faster initially but after a certain number of exothermic chemical reactions take place in the resin, the temperature of the resin begins to rise faster than that of the fiber. Therefore a thermal model based on heat induced in the material during cure by the energy of radiation as well as the exothermic chemical reactions of cure is to be developed to accurately estimate the temperatures and thermal properties during cure.

The heat induced during cure is dependent on the number of exothermic reactions taking place and hence on the cure kinetics of the system. The increase in the number of reactions taking place leads to an increase in molecular weight and temperature and this has an effect on the viscosity of the material.

In this thesis we study the characteristics of the Diglycidyl ether of bisphenol A - Diaryl iodonium hexaflouroantimonate (DGEBA - $I^+SbF_6^-$) resin-initiator system during electron beam curing and it's potential use in the aerospace industry. Basic models will be developed to determine the cure kinetics, temperature and viscosity.

Figure 3 shows a flowchart of the overall technical plan of the project.

```
┌─────────────────────────┐         ┌─────────────────────────┐              ┌──────────────────┐
│ Thermal curing of DGEBA –│        │ E-beam curing (0 – 150  │              │ DSC study of the │
│ I'SbF₆ system using DSC │         │ kGy) of DGEBA – I'SbF₆  │              │ initiator        │
│                         │         │ system with different   │              │                  │
│                         │         │ initiator concentrations│              │                  │
└─────────────────────────┘         └─────────────────────────┘              └──────────────────┘
```

Isothermal at 177 and 215 °C	Dynamically up to 250 °C	Chemical analysis using FTIR	T_g using DSC	Temperature versus time plots measured *in-situ*	Realization of Melting point and point of dissociation
Study of the effects of moisture, calculation of activation energy	Study of the effects of moisture on the cure rate	Calculation and analysis of cure rate at different doses with different initiator concentrations	Analysis and comparison with literature values obtained for thermal curing, discussion of possible reasons for lower values during e-beam curing	Analysis of plots	Comparison with temperatures during e-beam curing
Calculation of the cure rate at lower tmeperatures		Modeling the cure kinetics using above results and autocatalytic model	Analysis of reactions involving Ether and OH groups		

```
┌──────────────────────────────────┐
│ Modeling the heat induced in the │
│ material due to e- beam irradiation│
│ and exothermic reactions         │
└──────────────────────────────────┘
```

```
┌──────────────────────────────────────────────────────────┐   ┌──────────────────┐
│                    Potential to:                          │   │ All findings to be│
│ Calculate the molecular weight as a function of degree of cure, │ used in           │
│ Model the viscosity as a function of degree of cure and temperature,│ hygrothermal │
│ Calculation of equation constants                         │   │ model being      │
│ Conduct future research on the viscosity                  │   │ developed        │
└──────────────────────────────────────────────────────────┘   └──────────────────┘
```
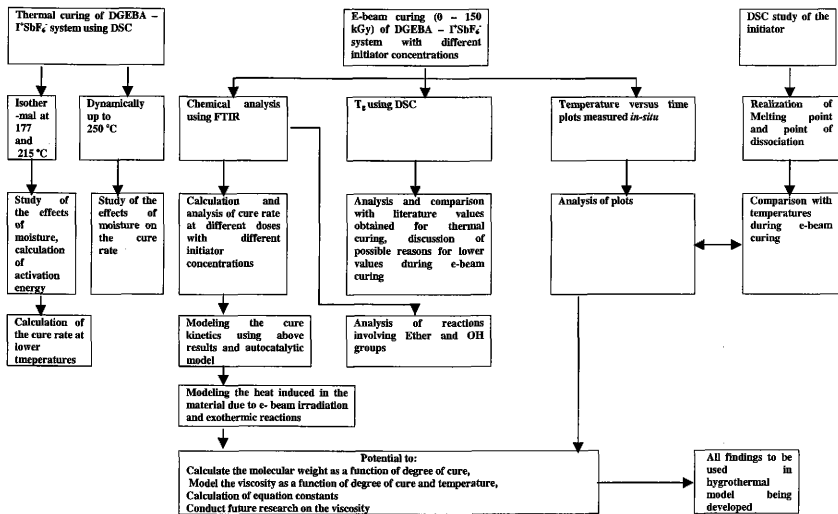
Figure 3. *Overall technical approach*

CHAPTER II

THEORY AND REVIEW OF LITERATURE

Structure and Curing of Epoxies

The curing of epoxy resin composites becomes the most important phase in developing acceptable properties in the final composite part. "Properly cured, the composite has many properties far superior than those of the classical materials. Improperly cured, the composite is of no use for structural applications and has no realistic function" [10].

An epoxy consists of molecules containing the 'epoxide' or 'oxirane' ring (refer to Figure 4) at both ends. During polymerization, this ring opens leading to the formation of chains and crosslinks.

In this thesis we study the curing and properties of the epoxy Diglycidyl Ether of Bisphenol A (DGEBA) which has the structure as shown in Figure 5.
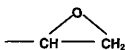
Figure 4. Chemical structure of the epoxide or oxirane ring
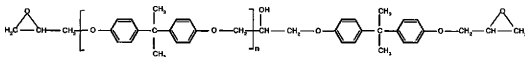
Figure 5. Chemical structure of diglycidyl ether of bisphenol A (DGEBA)

The epoxide group can bond chemically with other molecules, forming a large three-dimensional network. This process, called curing, changes a liquid resin into a solid. A number of curing agents exist such as:

Amines

These contain molecules having the NH_2 group at both ends. The nature of curing is as shown in Figure 6.
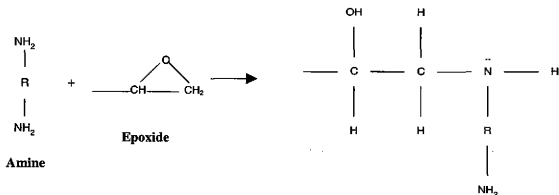
Figure 6. Curing of an epoxy with amine

Anhydrides

These react with epoxy resins to form esters. For the curing reaction to occur, the anhydride ring must be opened. The nature of curing is as shown in Figure 7.
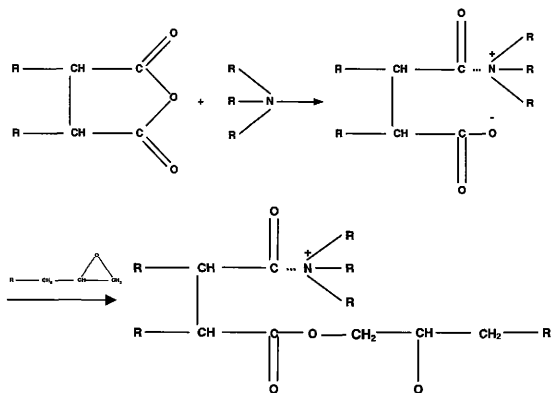
Figure 7. Curing of an epoxy with anhydride

Cationic polymerization using catalyts

Added in small amounts to the epoxy resin, a Lewis acid functions as a catalyst by cationically homopolymerizing the epoxy molecules. It has been discovered that diaryiodonium salts having complex metal halide counterions are efficient photoinitiators for the polymerization of a variety of cationically polymerizable monomers [11]. Diaryliodonium salts (having the general structure shown in Figure 8) are found to be more stable than dialkyliodonium and alkylaryliodonium salts and can

AR1 —————— I^+ ——————— AR2 ————— MX_n^-

AR1 and AR2 are aryl groups

I^+ is the iodonium ion

M is a metal

X is a halide

n is an integer value

Figure 8. General chemical structure of a diaryliodonium salt

be readily isolated and purified by conventional techniques [11]. Diaryliodonium salts are also found to be more effective initiators than the triarylsulfonium salts of the same anion [12]. Lopata et al. [13] showed that the cationic initiators can have a significant effect on the e-beam dose required to cure the epoxy resin as well as the resulting polymer's rheological properties. Within a given initiator family, the effective cure enhancement of anions is in the following order:
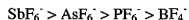
$$SbF_6^- > AsF_6^- > PF_6^- > BF_4^-$$

On exposure to high temperatures or e-beam irradiation, these anions are removed from the salts and form Bronsted acids with hydrogen containing compounds like water (refer to Figure 9). These Bronsted acids are the ultimate initiators when diaryliodonium salts are employed in the cationic polymerization of various monomers.

In this thesis we study the curing of DGEBA with initiators produced by the decomposition of onium salts containing the SbF_6^- anion resulting in the generation of the Bronsted acid $HSbF_6$ which acts as the precursor for polymerization (refer to Figure 9). This resin – initiator system was studied because it was the chosen system by the e-beam community as part of the Cooperative Research and Development Agreement (CRADA) program sponsored by the Department of Energy Defense Programs , through Oak Ridge National Laboratories.
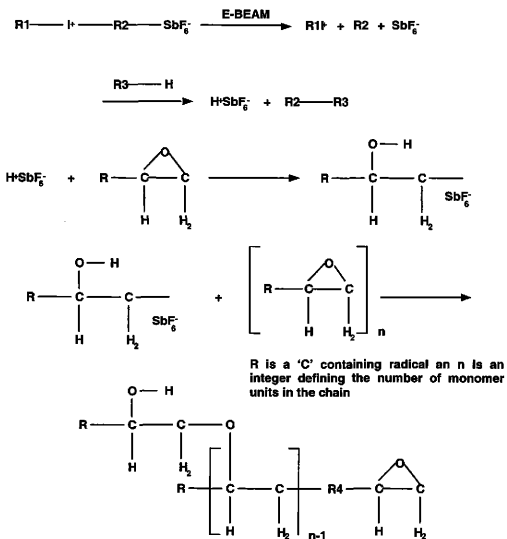
Figure 9. *Initiation and polymerization of the $I^+SbF_6^-$ - DGEBA initiator – resin system during electron beam curing*

Thermal Curing Details

So far the most popular method for thermoset curing has been the thermal method. It is more well developed and understood than the e-beam curing process. The cure characteristics of this method have been well understood and they form the basis for the study of the e-beam cure process. The thermal cure process is described in the following paragraphs.

Processing materials must be added to a composite ply lay-up before autoclave curing [14]. These materials control the resin content of the cured part and ensure proper application of autoclave pressure to the lay-up. A laminate lay-up prepared for autoclave curing is shown in Figure 10. The materials used in this method consist of a separator, bleeder, barrier, breather, dam, and vacuum bag. Separators are placed on top of and under the laminate. These release materials, which are usually fluorocarbon polymers, allow volatiles and air to escape from the laminate during cure, and they must be easily removed from the cured laminate without causing damage. The bleeder is incorporated to absorb excess resin from the lay-up during cure, thereby producing the desired fiber volume and part dimension. Fiberglass or other absorbent materials are used for this purpose. A non-adhering material, called the barrier, is commonly placed between the bleeder and breather. In the case of epoxy resins, it is frequently an unperforated film so resin removal from the part can be controlled. Sometimes a tool plate, called the gaul plate, is also placed between the bleeder and breather. The breather is a material placed on top of the barrier film to allow uniform application of vacuum pressure over the lay-up and removal of entrapped air. A dam is sometimes located peripherally to minimize edge bleeding. Finally, the vacuum bag is used to contain any vacuum pressure applied to the lay-up before and during cure and to transmit external autoclave pressure to the part [5].

The curing process is brought about by exposing the bagged lay-up to elevated temperatures and pressures for predetermined lengths of time. Cure has a

direct impact on the properties of the resin matrix and the performance of the final composite. The heat energy applied causes the matrix resin to melt and flow. It also provides the energy required for initiating and maintaining the crosslinking chemical reactions in the resin. The increase in temperature and the simultaneous changes in the molecular structure result in a decrease of the resin viscosity, enabling the resin to flow initially. The crosslinking reactions are exothermic in nature and therefore add to the heat provided by the autoclave. The reactions are also irreversible in nature, and result in an increase in molecular weight of the resin. The epoxy resin changes from a liquid to a rubbery state, and finally to a solid at the gel point. Beyond the gel point, the resin ceases to flow, and the shape and size of the composite get fixed. Before the resin gels, pressure is applied. Since each prepeg ply usually contains more resin than what is needed, the applied pressure provides the force needed to squeeze the excess resin out of the material and to consolidate individual plies. The pressure is also useful in forcing the resin to coat every fiber and in minimizing voids. Gases and water vapor can be entrapped in the composite during cure producing voids in the product, making it unusable [5]. The magnitude and duration of the temperature and pressure application, which is referred to as the 'cure cycle', significantly affects the performance of the finished product and the production rate.

The cure cycle affects the following parameters [5]:

- The temperature inside the prepeg
- The reaction rate and degree of cure of the resin
- The resin viscosity
- The resin flow
- The amount of resin in the prepeg and the amount of resin in the bleeder
- The changes in void sizes
- The residual stresses in the composite

The cure cycle thus must be selected carefully for each application to produce a structurally acceptable part. Some of the major considerations in selecting the proper cure cycle are [5]:
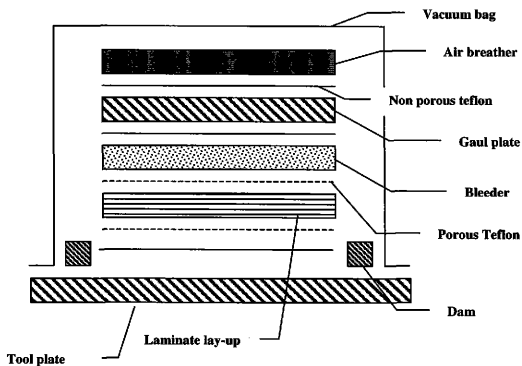
Figure 10. Components of a laminate lay-up for thermal curing

- The temperature inside the material must not exceed a preset limit during cure to prevent degradation
- The cure pressure must be sufficiently high so that excess resin is squeezed out from every ply of the composite before the resin gels at any point inside the composite, and must ensure that the resin coats every fiber and distributes uniformly
- The pressure must be applied while the viscosity of the resin is low enough to flow but not too low so that it is overly squeezed out

- The resin must be cured uniformly and completely to obtain ultimate mechanical properties
- The cured composite must have the lowest possible void content
- The curing process is achieved in the shortest amount of time

As the structural parts become larger, thicker, and more complex in contour in recent years, the cure process modeling has become much more important. Process modeling usually consists of representing the process under consideration by mathematical Equations and then solving them numerically on a computer to predict behavior. Once a process model has been constructed and verified, it can be used to explore the effects of systematically varying the process variables for different product geometries and to consider the changes in processing caused by altering material properties. Different process paths can then be proposed, analyzed, and compared by running the process model. The ability to predict the outcome of a given process path allows the engineer to determine the optimal process path and identify the critical variables that must be monitored to control the process properly. The ultimate use of the process modeling is the implementation of computer-controlled cure processes [5].

Electron Beam Curing Details

E-beam curing apparatus

A typical setup of electron beam curing equipment is shown in Figure 11. An electron beam 'gun' is either passed over the target material or the target material is passed through the beam, thereby covering the required surface area. The curing apparatus can be set up in several different ways providing radiation on one or both sides of the target material, different speeds of movement and localized curing. The unit used to quantify the energy absorbed by the target material exposed to an electron beam is the 'kilo Gray'. One kilo Gray (kGy) equals one kilo Joule per kilogram of target material.

An electron beam gun is also known as an accelerator. It consists of a cathode which is heated either directly by passing a current through it or indirectly by placing it next to a filament which is directly heated. The heat produced in the cathode is absorbed by the electrons present in it. When the energy of these electrons is greater than their threshold energy, they are able to overcome the attractive force of the nucleus and are ejected from the cathode. A number of such electrons are shaped into a beam
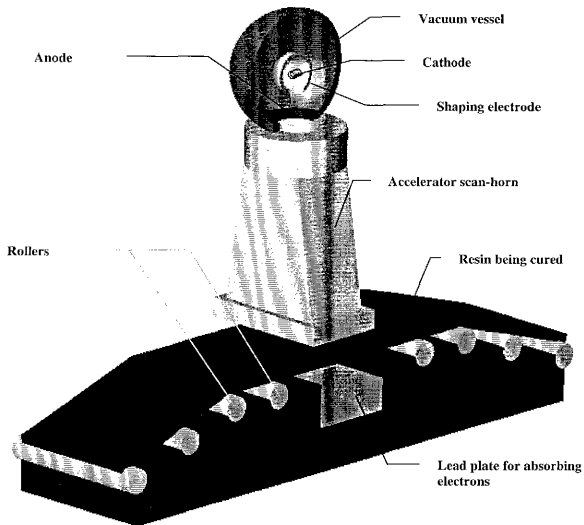
Figure 11. Electron beam curing facility setup

by a shaping electrode and are accelerated towards an exit window by an accelerating anode, hence the name 'accelerator'. The cathode is usually placed in a vacuum housing to prevent interaction of the electrons with any gas or vapor.

The interaction of high energy electrons with condensed materials depends on both the kinetic energy of the electrons and the atomic composition of the irradiated materials [15].

"The most useful 'penetration depth' is that up to which the dose is equal to the dose at the surface, which, for electron energies in the range 1-10 MeV, is given by:

$$d = \frac{0.4E - 1}{\rho} \tag{2}$$

Where E is the electron energy in MeV, and ρ is the average density of the material in g. cm^{-3}. This depth can be effectively increased by a factor of 2.4 by irradiating both sides of the material" [15].

Throughput is a function of the power of the electron beam [15]. In theory, 1 kW will process 3600 kGy kg.hr^{-1}. To this one must apply a factor for the efficiency of utilization of the beam. This will vary with the type of material being processed and the method of transportation of the product through the beam. Therefore, for treating insulated wire, the efficiency can be 10 to 15%, while for a thick sheet it may be as high as 80%.

Accelerators used for industrial processing in the energy range 0.5-10 MeV fall into two main groups: Direct Current (DC) and Radio Frequency (RF, also known as Continuous Wave, CW) linear accelerators (linacs) types. In the direct type, the full accelerating potential is developed across the terminals, this potential

being used to accelerate the electron stream. In the linac, the electrons travel in an RF electromagnetic field in which they are accelerated up to the desired potential [15].

An electron beam processing facility consists of six main elements [15]:

- Accelerator
- Product conveyor
- Radiation shield
- Ventilation system
- Safety system
- Control system

Accelerator

The depth of penetration is a function of the beam energy. Therefore it has to be related to the thickness and density of the product. A good match is required, both for ensuring adequate dosing of and dose distribution within the product, and for achieving optimum size and an economic performance of the facility.

"The beam energy can be varied on most DC accelerators by dial selection over a range of 3:1, with some loss of maximum output power. Such variation is more difficult to obtain with RF linacs, which suffer much more reduction in maximum power when moving away from the design beam energy level" [15]. Other ways of achieving proper treatment of the product, in spite of a mis-match of energy and thickness/density of the product, are by carefully designing the product handling equipment.

The benefits to be obtained from a good match between product and energy are [15]:

- Smallest possible cell size
- Lowest cell cost

- Optimum dose distribution in the product
- Optimum beam utilization efficiency

The beam power defines the theoretical maximum product throughput of the facility. Therefore, beam power choice affects the cost of the accelerator, size and cost of the product conveyor, size of the building (for storage of the finished product and the product awaiting processing) and the size of the ventilation system and incoming electrical mains supply. Overall, the cost per kW of beam power, and hence the unit cost of the finished product, will be lower with a higher power version of the accelerator with a particular beam energy rating [15].

Product conveyor

Products to be handled can be grouped into three categories [15]:

- Continuous (wire, sheet, tube etc.)
- Piece parts (molded parts, packages etc.)
- Other (bulk liquids, powders etc.)

Continuous products

These products are usually handled under the beam on an array of pulleys or rollers. The system is to be designed to present the product to the beam in such a way as to absorb the electrons fully and to achieve uniform distribution of dose across the product. Early 'underbeam' systems used arrays of pulleys, carrying the product either in 'racetrack' or 'figure of eight' configuration. These have been largely superceded by drum systems [15].

A small rotation of the product under the beam can make a substantial improvement in the uniformity of the dose distribution. The drum system produces sufficient rotation per pass to optimize the dose distribution in wire products [15].

The product can be wrapped round the drum system many times (up to 200 wraps per meter), giving an incremental dose on each pass, and enabling the product to be run at high speed.

It is important, particularly with heat shrink tubing, to minimize stretching of the product. The drums of the underbeam capstan are all driven, so that the capstan imposes no tension on the product. The tension is controlled in the transport system by 'dancers' [15], hydraulically or pneumatically operated, adjacent to the pay-off and take-up stands.

The underbeam capstan can also be used for handling sheet products, a big advantage in a service center facility. In some installations, the roller system inverts the sheet and passes it back through the beam upside down and in the opposite direction. For a thin sheet, it is desirable to multi-pass the sheet through the beam in order to improve the beam utilization.

In a high energy facility with large diameter cables, the size and stiffness of the conductor make it difficult to handle the product on an in-cell fixture and to achieve acceptable uniformity of dose distribution in the insulation. Two solutions are the drum-twister fixture, and the use of two accelerator heads [15]. In the first, the cable makes a single pass through the cell under the beam, rotating as it passes through the beam, so obtaining even dose distribution [16]. The rotation is achieved by using pay-off and take-up stands which rotate the drum as it is paid off and rewound. In the second case, a facility using two accelerators gives effectively four-side irradiation of the cable, which is passed several times, without twist, through the two beams which are off-set at 90° to each other [17].

Piece parts

Piece parts are handled by more conventional transport means such as roller conveyors, monorails or wheeled cart systems [15]. These systems, particularly the

latter two, usually have control systems that enable the user to pre-program the number of passes under the beam of each carrier or cart, to rotate the carrier to achieve automatically two side irradiation of the product and to identify the appropriate carrier or cart involved in any significant variation in beam characteristics during processing.

Other products

Other products, such as liquids and powders, need to have customized handling systems in order to be processed in bulk. They can be handled in suitable packages on a piece parts conveyor, but this is not very practical except for comparatively small volumes of product.

Powders can be handled effectively in a pneumatic transport system, with the underbeam section of the transport tube having a thin titanium window allowing entry of the electrons emerging from the accelerator scan horn. Liquids may be handled in a similar pumped system. Alternatively, a liquid can be pumped over an open weir placed under the electron beam, thereby achieving control of the depth of the product in order to ensure full penetration of the beam.

Radiation Shield

Adequate shielding is to be provided around the processing e-beam equipment in order to reduce the radiation outside the cell to below the permissible level. In order to design the required shielding, one needs to know the total radiation flux, the dimensions of the cell, and the attenuation characteristics of possible shielding materials.

The radiation flux has two elements - primary and secondary radiation [15]. Primary radiation is the electron beam from the accelerator. It has high intensity but relatively low penetration. Secondary radiation consists of X-ray photons generated

when the electrons collide with nuclei in the target material and cell equipment. These have reduced intensity but high penetration.

The choice of shielding material is governed by cost and cell layout considerations [15]. At fairly low voltages, comparatively thin sections of steel and lead are able to provide localized shielding. There should be provisions for adequate access to different parts of the cell for products, services and personnel.

Ventilation System

Some of the by-products of electron beam curing are X-rays and Ozone (ozone is produced by electrons interacting with air in the facility). After the accelerator is shut down, some time is given for the X-rays to lose their energy before personnel can enter the facility. The ozone that is produced is harmful above a particular concentration and it's concentration is reduced by providing fresh air inlets at one end of the cell with an exhaust at the other end so that the fresh air scavenges the ozone present, across the cell and reduces it's concentration.

Safety System

The safety system consists of devices for protection against high voltages, mechanical guards, and equipment for protection from radiation. Apart from radiation shielding we need devices to warn personnel against harmful radiation in the chamber.

Items that need to be included are [15]:

- Mechanical and electrical interlocks on all doors and entrances
- Sequenced key locks for the accelerator controls
- Visible warnings at entrances to the radiation area
- Audible warnings before the accelerator is switched on

- Visible warnings during accelerator operation

Control System

Stable and reliable operation is achieved by providing stabilized power supplies and fast acting solid state sensor and control devices. Control and monitoring systems help in achieving the following:

Required product treatment

This is achieved by providing the appropriate dose and dose distribution to the product material. Dose penetration can be affected by the orientation of the product in the beam. The required orientation can be obtained by dose mapping and other dose trials [15].

The applied dose is characterized by the product or gun speed, energy of the beam, beam current and width of the scanned beam. These are adjustable parameters that can be varied to obtain optimum dosage.

Safer operation

This is achieved using devices mentioned earlier under safety system.

Rectification of fault modes

During periods of faulty operation, parts of the product could remain 'underdosed' (not enough dose). The availability of micro-electronic devices has helped a great deal in the detection and correcting of fault modes of operation.

Dosimetry

This is the study of dose characteristics and their effect on properties of the product. In electron beam curing of composites it is necessary to optimize the dose intensity and the time of exposure, in order to obtain desired properties of the product.

A dosimeter is an instrument used to measure the amount of dose energy absorbed by a fixed volume (called sensitive volume) of product.

Important Irradiation parameter definitions

Beam Energy (MeV): Nominal energy of electrons at the accelerator exit

Beam spot (cm^2): The area that is irradiated, by the beam, at any given time. The edge of the beam spot is defined by the line where the dose rate is reduced to 10% of the peak dose rate at the center of the beam spot.

Beam length (cm): length of the beam as seen by a target moving along the conveyor. It is usually equal to the beam spot diameter.

Beam power (Watts): Power delivered by the beam at the scan horn exit integrated over a time period that is a positive integer multiple of the pulse period in pulsed accelerators. It is the product of beam current and beam energy.

Conveyor speed (cm/s): the speed at which the irradiation target is moved, by the conveyor, through the beam.

Illumination period, dwell period (s): The time period during which a specified point is being consistently irradiated.

Pass: Translation of the irradiation target, through the beam, one time.

Rest period (s): The time period between irradiations for a specified point in the irradiation target.

Absorbed dose (kGy): Amount of radiation energy absorbed per unit mass of irradiated material.

Dose rate (kGy/s): The rate of dose delivered during a specified time period.

Heat Transfer Models Developed

Modeling the heat transfer and chemical kinetics of the cure process of thermosets and their composites is a complicated task due to certain characteristics such as:

- Variable thermal properties with space and time
- Resin flow
- Void formation
- Presence of moisture and other impurities
- Multi dimensionality of properties
- Irregular dimensions

Process modeling is a handy tool for determining the material characteristics without the use of costly and time consuming experimental and trial and error procedures.

Finite difference methods are the most widely used techniques for the solution of fluid flow and heat transfer problems due to the ease of understanding, development and programming of the technique [18]. The main drawback of this technique lies in it's inability to accommodate complex boundaries. Large errors

appear if the boundary doesn't pass through the grid points. The errors arising at the boundary can propagate into the field and result in inaccurate solutions. The finite element methods eliminate this problem but at the expense of simplicity and ease of programming [18].

A new method of grid generation was developed by Chu [19] and further developed by Thompson et al [20]. This method, known as the Body-fitted co-ordinate (BFC) system, has eliminated the problem introduced by complex boundaries. The use of this system consists of two steps: the first is the transformation of the physical field into a rectangular computational field, and the second is the transformation and solution of the differential Equations describing the problem.

Description of some cure process models developed

Loos and Springer [21,22] developed models and created a computer code named "CURE" based on thermo-chemical and resin flow characteristics. The models include the determination of the temperature, pressure, and degree of cure as a function of position and time for a one-dimensional system.

The McDonnell Douglas model consists of five sub-models: heat transfer, fluid flow, voids, resin kinetics and viscosity [23].

Lockheed-Georgia developed a one-dimensional heat transfer code that can predict the temperature profile and viscosity as a function of position and time [23]. The code is known as "ROAST".

The model of Servais, Snide and Bern could predict the temperature profile through a laminate stack during the press-cure cycle [24]. It consisted of a one-dimensional, transient energy Equation, having a temperature dependent heat source and constant thermal properties.

Gutowski developed a flow/fiber deformation model [25]. Calius and Springer developed a computer code known as "WIND" that is structured in the same fashion as the "CURE" model of Loos and Springer. Pagano and Soni [26] described two models: Process Environment Model (PEM) and Mechanical Model (MIPAC). Lindt's [27] model consists of solving a set of equilibrium Equations for the fibers in order to describe the consolidation process. Kardos et al [28] presented the framework for a model that can predict void formation and transport during the cure of composite materials. Ma et al [29] developed a mathematical model to simulate heat transfer and the curing reactions of unsaturated polyesters in a rectangular die of a pultruder. Hou [30] developed an analytical model to predict viscosity during cure.

The general Equation governing the heat transferred to a material during electron beam curing is:

$$Q = D + q \qquad (3)$$

where:

Q is the total heat added to the material

D is the radiation energy

q is the internal heat liberated due to the exothermic chemical reactions

Chemical Reaction Kinetic Models Developed

The chemical kinetics or the rate of cure of thermoset resins can be divided into two main categories:

n^{th} order kinetics

The rate of cure is proportional to the concentration of material that has yet to react. The reaction function is given by the expression:

$$\frac{d\alpha}{dt} = A \exp(\frac{-E_a}{RT}).(1-\alpha)^n \tag{4}$$

where:

    A is the Collision factor

    E_a is the Activation energy of the reaction

    R is the Universal gas constant

    T is the Absolute temperature

    α is the Degree of cure

    t is the time of exposure

    n is the order of reaction

Autocatalytic kinetics

The kinetics of autocatalyzed reactions are given by the expression:

$$\frac{d\alpha}{dt} = k.\alpha^m.(1-\alpha)^n \tag{5}$$

where m and n are both reaction orders and

$$k = A.\exp(\frac{-E_a}{RT})$$

Sometimes the kinetics follow trends of both nth order and autocatalytic types and the rate expression is given by:

$$\frac{d\alpha}{dt} = (k_1 + k_2.\alpha^m).(1-\alpha)^n \tag{6}$$

where k_1 and k_2 are the rate constants

The models mentioned above were derived to characterize the kinetics of autoclave cured thermoset resins. The reaction kinetics of electron beam cured thermoset resins are not understood well. However they are found to exhibit reaction kinetics very similar to that of autoclave cured resins.

Kaetsu et al [31] conducted investigations on radiation-induced polymerization of hydroxyethyl methacrylate (HEMA) and glycidyl methacrylate (GMA). They found that the initial polymerization rate was proportional to the 0.5 power of the dose rate in the region of relatively high temperatures and the dose rate exponent changed sharply to 1.0 at a temperature at which the viscosity of monomeric systems reached 10^3 centipoise.

Viscosity Models Developed

Viscosity of a thermoset during cure is a function of:

- Temperature (which is a function of time) and
- Molecular weight (which is a function of degree of cure)

Two theories used are:

- Branching theory and
- Concept of free volume

Branching Theory

Studies conducted by Flory [32] and Stockmayer [33] led to their development of mathematical expressions describing the growth of a three-dimensional network as a function of monomer type, quantity and functionality. The increase in viscosity can be directly attributed to the formation of crosslinks between monomer units [32]. Lipshitz and Macosko [34] combined the works of Flory and

Stockmayer and defined an expression for the increase in molecular weight as a function of cure with time-temperature-viscosity data of a thermoset to obtain a general expression of the form:

$$\ln \eta = \ln A + s.\ln \left(\frac{\overline{MW}}{MW_0} \right) + \frac{\left[D + C \ln \left(\frac{\overline{MW}}{MW_0} \right) \right]}{RT}$$ (7)

which can be written as:

$$\ln \eta = \ln A + \frac{D}{RT} + \left[s + \frac{C}{RT} \right] \ln \left(\frac{\overline{MW}}{MW_0} \right)$$ (8)

Where:

η is the viscosity at a particular time in poise

A, s, D, C are constants found by data fitting

$\overline{MW}$ is the weight average molecular weight of resin at a particular time

MW_0 is the molecular weight of the resin at zero conversion

R is the universal gas constant

T is the absolute temperature at a particular time

Macosko and Miller [35] derived the following expression for the molecular weight as a function of extent of reaction based on Stockmayer's molecular weight expression:

$\overline{MW}$ as a function of degree of cure for an epoxy-amine curing situation is given by:

$$\overline{MW} = \frac{P_e m_a' + P_a m_e'}{P_e m_a + P_a m_e} + \frac{P_a P_e [P_e (f_a - 1) M_e^2 + P_e (f_e - 1) M_a^2 + 2 M_a M_e]}{(P_e m_a + P_a m_e)[1 - P_a P_e (f_a - 1)(f_e - 1)]}$$ (9)

where:

P_a, P_e are extent of reactions (degree of cure) of amine and epoxy respectively

f_a, f_e are average functionalities of amine and epoxy respectively

$$m_a = \frac{\sum_i M_{Afi} A_{fi}}{\sum_i f_i A_{fi}} \text{ and } m_a^{'} = \frac{\sum_i M_{Afi}^2 A_{fi}}{\sum_i f_i A_{fi}}$$

$$M_a = \sum_i M_{Afi} a_{fi} \qquad (10)$$

where:

$$M_{Afi} = f_i M_c$$

where:

M_c is the weight between cross-linkable sites and end chain end weight is assumed to be $M_c / 2$

f_i is the functionality of amine monomer of type denoted by subscript i

A_{fi} is the number of moles

$$a_{fi} = \frac{f_i A_{fi}}{\sum_i f_i A_{fi}} \qquad (11)$$

$m_e, m_e^{'}$ and M_e are similarly defined.

For the curing of a pure epoxy with a single type of monomer we have:

$$\overline{MW} = \frac{m_e^{'}}{m_e} + \frac{P_e M_e^2}{m_e[1 - P_e(f_e - 1)]} \tag{12}$$

Extent of cure P_e which is usually symbolized by α as described earlier.

Free Volume Concept

The Equation for viscosity at a particular time *(t)* and temperature *(T)* is given by the following Williams-Landel-Ferry (WLF) [36] Equation:

$$\log \eta(t) = \log \eta(T_g) - \frac{C_1(T - T_g)}{C_2 + (T - T_g)} \tag{13}$$

where:

$\eta(T_g)$ = viscosity at glass transition temperature T_g

$\eta(T_g)$ and T_g are functions of degree of cure

C_1 and C_2 are constants irrespective of temperature

Modeling the Viscosity as a function of Degree of Cure and Temperature:

Lee et al [37] conducted studies on the heat of reaction, degree of cure, and viscosity of Hercules 3501-6 resin using a differential scanning calorimeter and disc and plate type viscometer. They derived the following expression relating the viscosity to the degree of cure and temperature:

$$\eta(T, \alpha) = \eta_0 \exp\left(\frac{U}{RT} + K\alpha \right) \tag{14}$$

where:

η_0 is a constant

U is the activation energy for viscosity

K is a constant independent of temperature

CHAPTER III

EXPERIMENTAL DETAILS

Materials

Material tested and characterized

       Industry name: Epoxy resin Tactix 123.

       Chemical name: Diglycidyl Ether of Bisphenol A (DGEBA)

       Structure: As shown in Figure 5

       Epoxy equivalent weight: 172-176
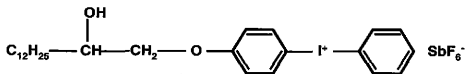
       Manufacturer: Dow chemical company

Initiator

       Industry name: SarCat CD 1012

       Chemical name: Diaryl Iodonium Hexaflouroantimonate

       Structure: As shown in Figure 12

       Manufacturer: Startomer

Figure 12. Chemical structure of diaryliodonium hexafluoroantimonate

Curing Details

The cure process takes place in the following steps (refer to Figure 9):

- *Photolysis of the initiator:* The initial structure of the initiator is as shown in Figure 12. On exposure to electron beam irradiation, it is split forming a positive and a negative charged species.

- *Forming a Bronsted acid:* The SbF_6^- ion reacts with 'H' containing compounds to form the Bronsted acid $H^+SbF_6^-$ which initiates the reaction.

- *Beginning of cationic polymerization:* The electron deficient H^+ has more affinity for the 'O' atom on the epoxide group and splits open the epoxide ring, leaving the 'C' atom at the end of the monomer short of two electons.

- *Propagation:* This electron deficient 'C' atom, in turn, breaks open the epoxide ring of other monomers leading to homopolymerization as shown.

- *Effect of counteranion:* The counteranion SbF_6^- is held electrostatically near the end of the chain and has a steric influence on the addition of monomer units.

E-beam Curing Setup and Details

The accelerator used for this experiment was an I-10/1 (10 MeV, 1 kW) electron accelerator. The experiment was performed by Vince Lopata at Acsion Industries Incorporated, Pinawa, Canada. The samples were filled in transparent syringes as shown in Figure 13. Different doses were applied to different samples (5,10, 25,50, 100 and 150 kGy). For each set of doses, different concentrations of the initiator were used (0.1, 1.0, 3.0 and 10.0 phr). The dose increment was 1 kGy/pass and the dose rate was 6.3 Gy/sec. A schematic of the experimental setup is shown in Figure 13.
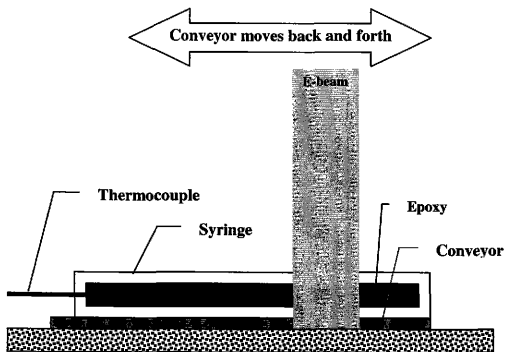
Figure 13. Schematic of the e-beam experimental setup

Differential Scanning Calorimetry (DSC) Details

The instrument used was a Perkin-Elmer Pyris 1 differential scanning calorimeter. The experiments were conducted at the Polymer Technology Center, Texas A&M University. A schematic of the apparatus is shown in Figure 14. The weight of the samples tested was approximately 20 mg. The tests were conducted in the dark to prevent further reaction from taking place. Dynamic tests were carried out on specimens to determine the residual exotherm and Glass Transition Temperature (T_g). The samples were scanned from 0 to 250 °C at a rate of 10 °C/minute. Isothermal cure was also conducted on uncured specimens at 177 °C and 215 °C to observe the effects of temperature and moisture on the cure rate.

In DSC we heat two pans simultaneously. One pan contains the polymer sample while the other is left empty. The heating is controlled by a computer such that the temperature of the two pans remains the same. A fixed heating rate is specified before starting the experiment (eg. 10 °C/min.). The rate of heat supplied to the sample pan is more than that of the reference pan as we have to heat the pan as well as the sample (unless the heating causes exothermic reactions causing the sample to heat up on its own, as in the case of an epoxy). While this heating goes on, we make a plot with the temperature on the X-axis and the difference in heat supply from the two heaters on the Y-axis.
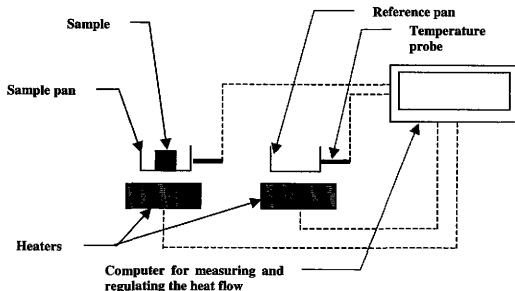
Figure 14. Schematic of the DSC apparatus

At the glass transition temperature we get a plot as shown in Figure 15. There is a sudden change in heat capacity at the glass transition temperature (T_g) as more heat can be absorbed due to greater molecular motion per °C rise in temperature.

When polymers reach a certain temperature above the T_g they have enough energy to orient themselves into crystalline arrangements. On forming stable crystals

they give off heat and hence the heat flow to the sample pan is reduced. The DSC plot shows the heat given out by the material as a peak in the curve and heat absorbed as a dip (refer to Figure 15). This temperature at which crystallization takes place is called the temperature of crystallization (T_c). Since heat is given out it is called an exothermic transition.

To make the reverse process take place we have to supply heat (latent heat) to the crystals to make them dissociate. The temperature at which this takes place is called the melting temperature T_m and shows up as a dip in the DSC plot (refer to Figure 15). Since heat is absorbed it is called an endothermic transition.
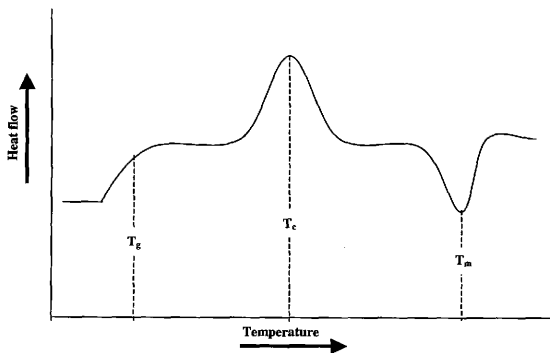
Figure 15. *A typical DSC plot showing glass transition temperature, temperature of crystallization and melting temperature*

Figure 16 shows an actual experimental DSC plot of the sample having 1 phr of initiator and dosed with 50 kGy. The heating rate was 10 °C/min. We can see a

marked change in heat capacity between temperatures of 72 and 82 °C giving a T_g value of 77 °C.
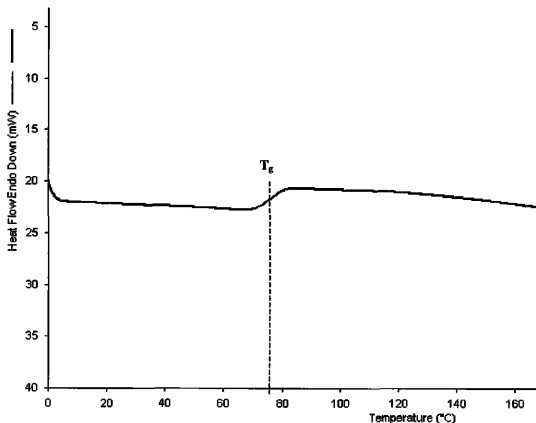

Figure 16. Actual DSC plot of the sample with 1 phr initiator and dosed with 50 kGy.

Fourier Transform Infra Red (FTIR) Test Details

Infra-red rays are electro magnetic rays with wavelengths between 0.7 and 500 μm or wavenumbers from 20 cm^{-1} to 14,000 cm^{-1}. In a molecule, the atoms undergo twisting, bending, rotating and vibrational motions about their bonds. When these vibrations interact with infrared radiation, portions of the radiation are absorbed at particular wavelengths. The multiplicity of vibrations occurring simultaneously

produces a highly complex absorption spectrum, which is uniquely characteristic of the functional groups comprising the molecule and of the overall configuration of the atoms as well. A schematic of the FTIR experiment is shown in Figure 17. As indicated, an IR beam consisting of rays with particular wavelengths enters the sample. Some of the rays are absorbed completely and some partially by the sample. The detector detects the rays and their intensities as they exit the sample. A computer then subtracts the output from the input and displays the different wavelengths absorbed, along with their intensities. A sample plot of an FTIR spectrum used in our investigation is shown in Figure 18. The epoxide, ether and phenyl group peaks are indicated and their structures are shown below the plot.
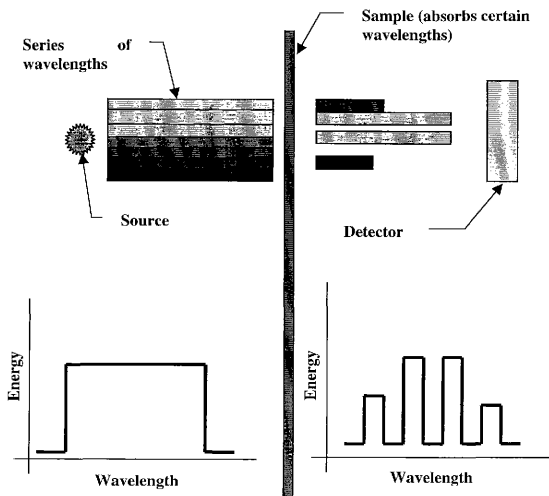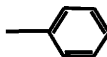
Figure 17. Schematic of the FTIR experiment
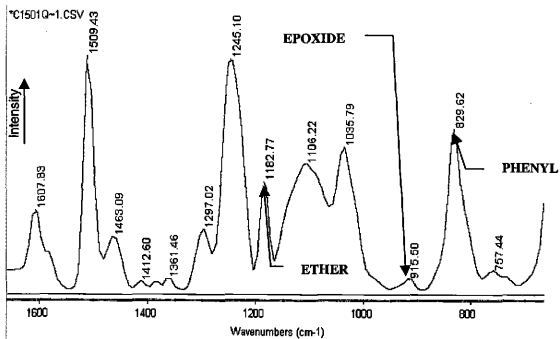
Figure 18. FTIR plot of resin sample dosed with 150 kGy e-beam irradiation and 1.0 phr initiator. Epoxide, Ether and Phenyl group peaks have been indicated.

The instrument used for these tests was a Nicolet Avatar 360 FTIR spectrometer. The experiments were conducted by Leila Bonnaud at the Polymer Technology Center, Texas A&M University. These experiments were also conducted in the dark to prevent further reaction from taking place. The partially cured specimens were in solid, transparent form. Different parts of each specimen were exposed to the IR rays and the average reading was taken.

The different groups investigated and their corresponding wave numbers are:

Epoxide: 900 to 950 cm^{-1}
Ether: 1090 or 1180 cm^{-1}
Hydroxyl: 3150 to 3625 cm^{-1}

The epoxide and ether group intensities were normalized to the phenyl group intensity from 800 to 840 cm^{-1} and the hydroxyl group intensity was normalized to the phenyl group intensity found from 1600 to 1650 cm^{-1}. The phenyl groups are assumed to be chemically unmodified during the cure process.

The following relation was used in determining the amount of epoxy conversion:

$$\alpha(D) = 1 - \frac{h_{epoxy(D)}/h_{phenyl(D)}}{h_{epoxy(D=0)}/h_{phenyl(D=0)}} \tag{15}$$

where:

$\alpha(D)$ is the epoxy conversion for a dose of D kGy

$h_{epoxy(D)}$ is the intensity of the epoxy band at dose D

$h_{phenyl(D)}$ is the intensity of the phenyl band at dose D

$h_{epoxy(D=0)}$ is the intensity of the epoxy band of uncured sample

$h_{phenyl(D=0)}$ is the intensity of the phenyl band of uncured sample

CHAPTER IV

DATA ANALYSIS AND DISCUSSION

Degree of Cure versus Dose for Different Initiator Concentrations

Studies were conducted on the degree of cure of the resin at different doses to determine the effects of the e-beam and initiator concentration on the cure rate. Figure19 shows the percentage of epoxy groups converted at different e-beam doses (5,10,25,50,100,150 kGy) from the FTIR tests. The tests were conducted on samples containing different initiator concentrations (0.1, 1.0, 3.0, 10.0 phr). From the plot we can see that most of the curing takes place within the first 10 kGy of dosage for all initiator concentrations. The shape of the plot indicates that the conversion follows a typical arrhenius curve for autocatalytic kinetics. As the number of reactive species gets consumed, the conversion rate decreases and at the latter stages, is diffusion controlled. There is very little conversion beyond a total dose of 50 kGy. The total conversion increased with the increase in initiator concentration confirming the fact that the higher the number of initiating centers for reaction, the greater the chance of chain formation. However for the case with initiator concentration of 10 phr, the degree of cure at 5 kGy showed a lower value than the corresponding values at 1 and 3 phr but beyond a dose of 10 kGy the values were higher. This indicates that there is an excess of initiator at a concentration of 10 phr, causing aggregation of the initiator based on solubility limitations, at the initial stage. After polymerization is initiated and the temperature is increased, the separation and mobility of the initiator species increases leading to a higher reaction rate as compared to concentrations of 1 and 3 phr.

The maximum conversion achieved was 94% for the sample containing 10 phr of initiator concentration after being dosed with 150 kGy of e-beam irradiation and the maximum temperature of the same sample recorded was 76 °C. This gives an indication of the effectiveness of the e-beam method of curing at lower temperatures.
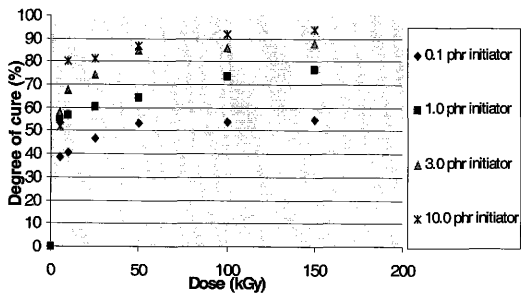
Figure 19. Percent conversion of epoxy versus dose

Rate of Cure versus Dose for Different Initiator Concentrations

The cure rate was calculated from the degree of cure versus dose information explained previously. This information is useful in modeling the cure rate at different doses and initiator concentrations. Figure 20 shows the rate of epoxy conversion at different doses (5, 10, 25 and 50 kGy) for different initiator concentrations (0.1, 1.0, 3.0 and 10.0 phr). There is a sharp increase in the rate up to a dose of 5kGy. The rate is higher for increasing initiator concentration except for the sample with 10 phr initiator concentration. Beyond this the rate decreases with increase in dose and beyond a dose of 25 kGy there is very little change in the reaction rate indicating that the rate is diffusion controlled beyond a certain degree of conversion. At this later stage of curing, the cure rate is almost identical for all initiator concentrations and hence can be considered to be independent of initiator concentration. Also the reaction rate is a function of remaining reactive species, therefore the reaction rate decreases as the reactive groups get consumed and the resin approaches the gel point. Here also we can see that the reaction rate is initially lower for the sample with 10 phr initiator but from a dose of 5 to 25 kGy it is much higher than the samples having lower concentrations of initiator. Therefore for controlling the reaction rate we have to determine accurate 'initiator-dose-reaction rate' relationships by conducting future experiments with a wide range of initiator concentrations and dose rates.
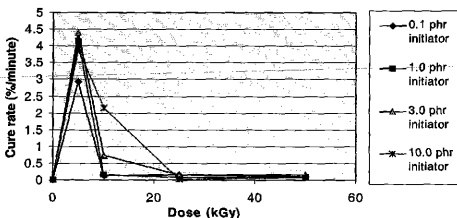

Figure 20. Rate of cure at different doses

Effect of Initiator Concentration on the Reaction Rate

We plotted the cure rates at different initiator concentrations at doses of 5 and 10 kGy in Figure 21. This information is useful in determining the effect of initiator concentration on the cure rate at different doses. For a dose of 5 kGy, there is a sharp increase in the reaction rate up to an initiator concentration of 1.0 phr assuming that no reaction takes place when there is no initiator. Beyond an initiator concentration of 1.0, the increase in cure rate is much lower per phr increase in initiator concentration. This indicates that we can choose an optimum value for the initiator concentration. A peak cure rate of 10.96 %/kGy for an initiator concentration of 1.0 phr indicates the small percent of initiator required to initiate the reactions. As mentioned and explained earlier, we can see the reaction rate decreasing for an initiator concentration of 10 phr at 5 kGy. At 10 kGy the reaction rate for 10 phr initiator is much higher than the rates for lower initiator concentrations compatible with the 'higher initiator concentration - higher reaction rate' trend.
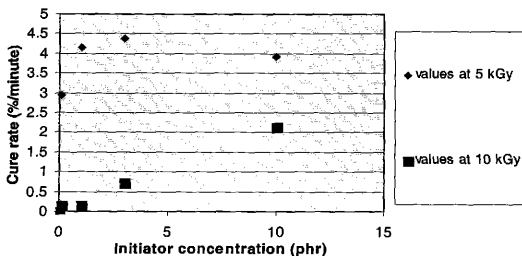

Figure 21. Change in the rate of cure with increase in initiator concentration

Rate of Heat Liberated versus Time at Different Temperatures Extrapolated from Isothermal DSC Results

From higher temperature, thermal cure, isothermal DSC experiments, we can extrapolate to lower e-beam cure temperatures, the rate of heat evolution. These plots give us an indication of the cure rate at lower e-beam curable temperatures. It is assumed that the effect of the e-beam on cure is only the activation of the catalyst initiator and the reactions take place as a function of temperature as in thermal curing.

DSC studies of the cure of the $I^+SbF_6^-$ - DGEBA initiator - resin system (initiator concentration is 2 phr) at temperatures of 177 ^{o}C and 215 ^{o}C (refer to Figure 22) showed peak exothermic rates of 0.65 and 1.886 W/g. Substituting these values in the reaction kinetic formula:

$$\frac{dH}{dt} = -A\exp(\frac{-E_a}{RT})f(x) \tag{16}$$

where:

$\frac{dH}{dt}$ is the rate of heat liberated in W/g

A is the collision factor

E_a is the activation energy for the reaction in kJ/kg

R is the universal gas constant

T is the absolute temperature and

$f(x)$ is a function of the number of available reactive species x,

we get the activation energy E_a as 59.1873 kJ/kg of resin.

Substituting this value in Equation (16), we get the approximate rate of heat liberated and hence the cure rate at lower e-beam curable temperatures (refer to Figure 23). This information is useful in modeling the heat induced in the resin and the resultant temperature during cure.
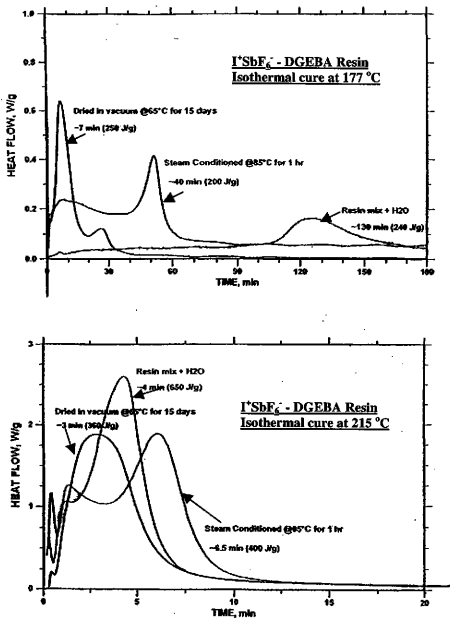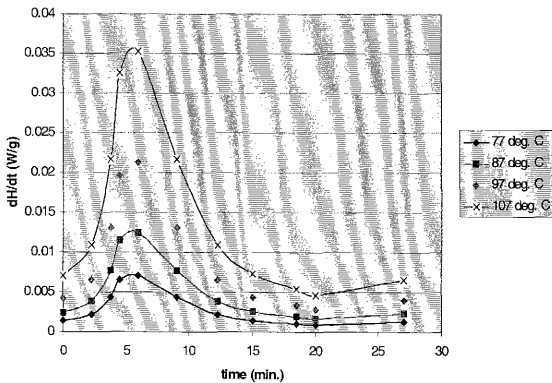

Figure 22. *Isothermal DSC plots of $I^{+}SbF_{6}^{-}$ - DGEBA resin system at $177\,^{o}C$ and $215\,^{o}C$*

Figure 23. *Rate of heat liberated versus time at different temperatures extrapolated from isothermal DSC plots at 177 °C and 215 °C*

Effect of Moisture on the Initiator

We studied the effect of moisture on the catalytic activity of the initiator from dynamic and isothermal DSC experiments. In Figure 24, DSC plots of initially dry and wet $I^+SbF_6^-$ - DGEBA resin system (2 phr initiator concentration) are illustrated. Most of the curing takes place in the 200-220 °C temperature range as a result of the dissociation of the $I^+SbF_6^-$ into active species. The initially moist unreacted resin was pretreated for one hour at 85 °C, 100 % RH. This caused a 6 °C shift to higher temperatures in the cure exotherm maximum as compared to the initially dry unreacted resin. The general trend is a doubling in the reaction rate for a 10 °C temperature increase. Therefore our finding indicates that the dissociation rate is reduced by 30 % due to the presence of moisture.

Referring back to Figure 22, we see the isothermal DSC curves at 177 °C and 215 °C for the $I^+SbF_6^-$ - DGEBA resin system. Three types of samples were tested. One was dried in vacuum at 65 °C for 15 days to minimize moisture, one was steam conditioned at 85 °C for one hour and the third was a mixture of the resin and water.

For the initially dry resin, the peak reaction rate was reached within 3 minutes for the test at 215 °C as compared to 7 minutes for the test at 177 °C. This gives an indication of the temperature dependence of the cure rate. The peak reaction rate for the other two cases also were reached in a considerably shorter period, for the test at higher temperature. For the curing at 177 °C, the peak reaction rate for the dry resin was reached in 7 minutes whereas the peak reaction rate for the resin mixed with water was reached in approximately 130 minutes. Therefore there is considerable slowing down of the reactions caused by the absorbed moisture. This indicates serious poisoning of the $I^+SbF_6^-$ catalyst activity by exposure to moisture even at the high thermal cure temperatures.

As the e-beam curing takes place below 100 °C, there is less chance of moisture escaping due to evaporation and therefore trapped moisture can

dramatically slow down the reactions and also lead to early chain termination. This causes poor crosslinking and a low molecular weight network as explained by Palmese et al. [38]. It can also lead to modification of the catalyst.
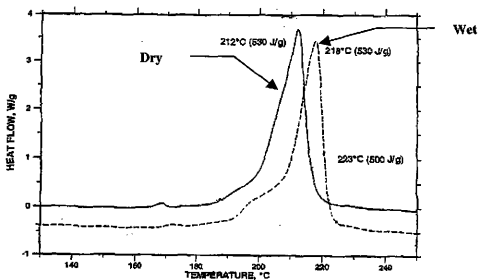
Figure 24. Dynamic DSC plots of initially wet and dry DGEBA – I⁺SbF₆⁻ resin – initiator system

DSC Study of Initiator

Dynamic DSC studies were carried out on the $I^+SbF_6^-$ initiator to determine the melting point and the temperature at which dissociation takes place. Figure 25 illustrates a DSC plot of the $I^+SbF_6^-$ initiator. It exhibits a melting point in the 94 - 100 °C range. There is an exotherm - endotherm at 205 °C, which is associated with the thermally–induced dissociation of the catalyst into active catalytic species for epoxide homopolymerization. It then forms the Bronstead acid $HSbF_6$ on reaction with 'H' containing compounds. This temperature of dissociation is in agreement with Figure 24 wherein the peak reaction rates are found between 200 °C and 220 °C.
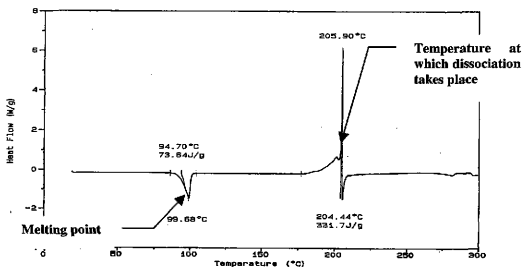

Figure 25. DSC study of initiator

Temperature versus Time

The temperature during cure was measured *in-situ* to study the amounts and effects of heat induced in the resin during e-beam cure. Figures 26 (a) and (b) show the temperatures (measured with a thermocouple as shown in Figure 12) at total doses of 25 and 150 kGy for different initiator concentrations. In both cases the maximum temperature increases and is achieved in a shorter time with increase in initiator concentration except for a concentration of 10 phr where the maximum temperature is brought about in a longer period of time as compared to a concentration of 3 phr. This finding is compatible with the reaction rate information mentioned earlier. At the initial stages of curing with an initiator concentration of 10 phr, there is aggregation of the initiator based on solubility limitations. After polymerization is initiated and the temperature is increased, there is greater mobility of the initiator species leading to a higher reaction rate and hence a higher temperature as compared to concentrations of 0.1, 1 and 3 phr. At the temperature peaks, the exothermic reaction rates are high. At later stages of cure the temperature in the resin is due to e-beam irradiation alone and reaches a fairly low value. This indicates that most of the heat induced in the resin is due to the exothermic chemical reactions and a small percentage is due to e-beam irradiation.

The bottom picture of Figure 27 shows a close-up view of the temperature versus time plot, measured with a thermocouple, for an initiator concentration of 1.0 phr and total dose of 25 kGy. The plot has a wavy pattern as can be clearly seen. This is due to the heating and cooling during each pass of the specimen in front of the beam. The top picture shows a single specimen with a particular selected spot on it (indicated by a circle). As the spot passes through the beam, it heats up causing the temperature to rise due to the beam energy and exothermic reactions. After passing through the beam, the spot goes through a period of cooling before passing through the beam once again. The solid line plot shows the temperature increasing during the beginning stages of curing when the cure rate is high. The broken-line plot shows the

temperature decreasing during the later stages of curing when most of the reactive species are consumed and the resin approaches the gel point.
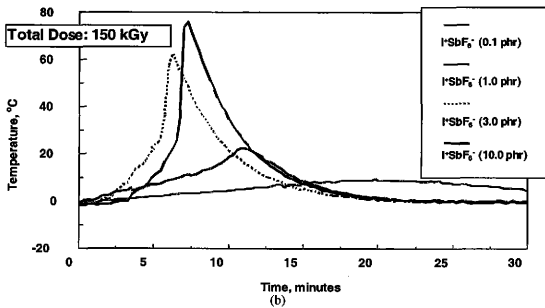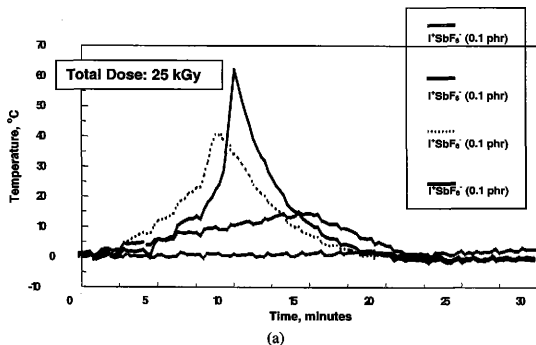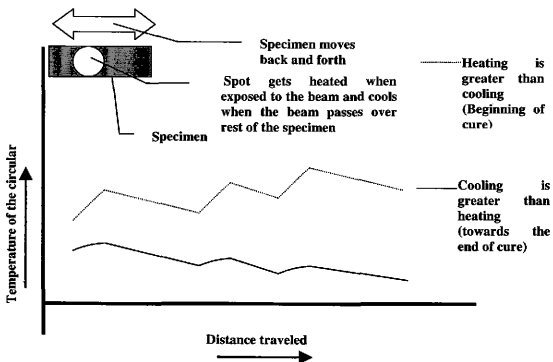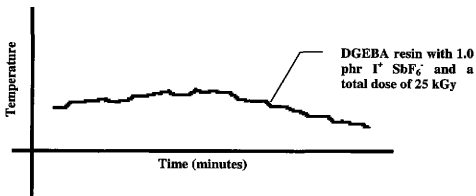

Figure 26. In – situ temperature versus time plots at doses of 25 and 150 kGy

Temperature of a beam spot during e-beam curing

In-situ temperature measurement during cure
using a thermocouple, showing a wavy curve

Figure 27. Analysis of the temperature profile during e-beam cure

Glass Transition Temperature (T_g) versus Dose

One of the goals of this project is to obtain a glass transition temperature in excess of 200 °C using e-beam curing. We studied the variation in T_g with dose to study the effects of dose and initiator concentration on the glass transition temperature and determine possible means of increasing it's value. Figure 28 shows the variation of the glass transition temperature of the e-beam cured I⁺SbF₆⁻ - DGEBA resin system with total dose, for different initiator concentrations. The T_g was observed from dynamic DSC tests as explained earlier under 'Experimental Details'. The T_g reached a maximum value of 86 °C at a conversion of 94 % for a dose of 150 kGy and an initiator concentration of 10.0 phr. The value of T_g, like the degree of cure, increased with increase in dose and initiator concentration. This confirms the dependence of T_g on the molecular weight and crosslink density. Defoort et al [39] found that for the same epoxide – initiator system cured thermally, the T_g obtained was 170 °C. This indicates that moisture or other 'H' containing impurities present at e-beam cure temperatures, induce chain termination reactions which reduce the crosslinks in the network leading to lower molecular weight and hence a lower T_g as explained by Palmese et al [38].
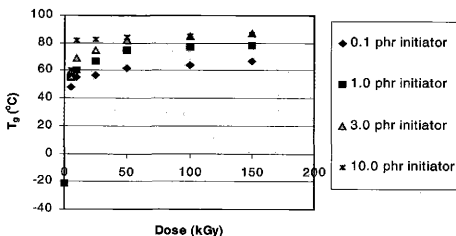
Figure 28. Glass transition temperature versus dose for different initiator concentrations

Reactions Involving Ether and OH Groups

From FTIR studies, we obtained the intensities of Ether and 'OH' groups at different doses and initiator concentrations. This was done to determine the effect of moisture or other 'H' containing compounds on the polymerization of the resin. Figure 29 shows the concentration of ether groups at different doses during the e-beam cure process. The concentration appears to increase and decrease in a sinusoidal fashion. Figure 30 shows the concentration of OH groups at different doses and it appears to increase initially, then decrease and finally stabilizes. The nature of the reactions causing this finding can be explained as shown in Figure 31. The epoxy reacts with water or other 'H' containing compounds forming 'OH' groups. These 'OH' containing molecules react with other epoxide containing molecules to terminate growing chains as shown in reaction (2) of Figure 31. Finally these macromolecules containing 'OH' groups react forming the R-O-R bond, releasing water. Finally the polymerization reaction of epoxy with epoxy gives an ether bond. These reactions give an indication of possible early chain termination and fewer crosslinks, causing a lower T_g.
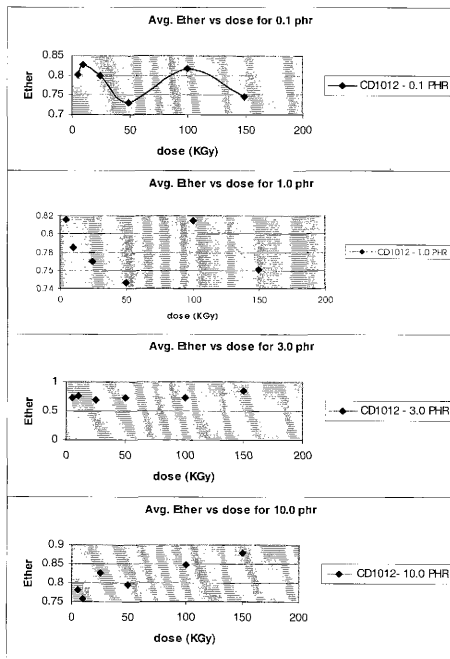
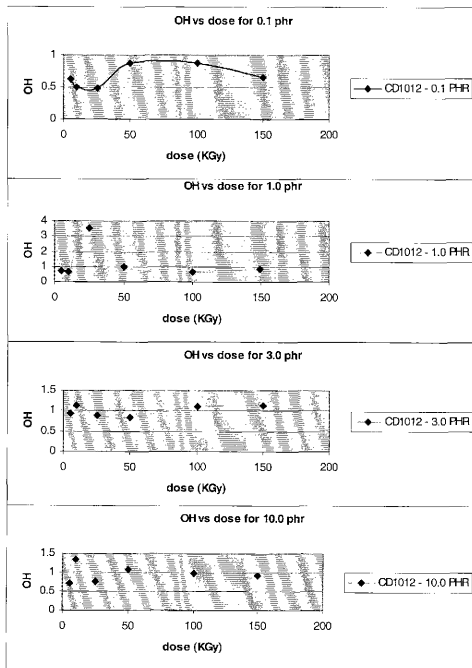**Figure 29.** *Change in ether concentration with increase in e-beam dose*

Figure 30. *Change in hydroxyl concentration with increase in e-beam dose*

$$R - CH \overset{O}{\underset{}{\diagup \diagdown}} CH_2 + H_2O \longrightarrow R - \overset{OH}{\underset{}{CH}} - CH - OH \qquad (1)$$

$$R_1 - O + R_2 - CH \overset{O}{\underset{}{\diagup \diagdown}} CH_2 \longrightarrow \left[R - \overset{O}{\underset{R_3, R_4}{CH}} - CH_2 - OR \right] \qquad (2)$$

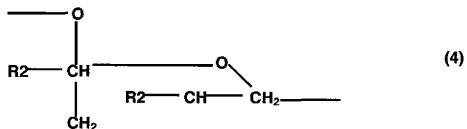$$R_3 - OH + R_4 - OH \longrightarrow R_3 - O - R_4 + H_2O \qquad (3)$$
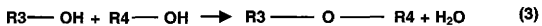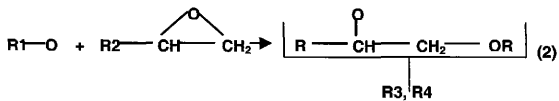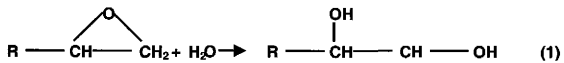
$$(4)$$

*Figure 31. Reactions involving ether and OH groups*

CHAPTER V

MODELING THE CURE KINETICS, HEAT TRANSFER AND VISCOSITY DURING CURE

The values for the cure kinetics, heat induced and viscosity were simulated for one gram of specimen material and were considered uniform over the whole specimen.

Modeling the Cure Kinetics During Cure

The autocatalytic cure model was used to model (i) the cure rate as a function of the degree of cure and (ii) the cure rate versus dose plot. The plots for the experimental and modeled values match very closely as can be seen in Figure 32. This confirms the autocatalytic nature of the cure reactions.

We used the cure rate values of the specimen cured with 10 phr initiator. Substituting values for the dose rate and the degree of cure in Equation (5), the values obtained for k, m and n are 3.9819 x 10^{111} (minute^{-1}), 253.0943 and 126.7879 respectively. The reaction constant k is a function of temperature but is assumed to remain fairly constant over the temperature range of cure.
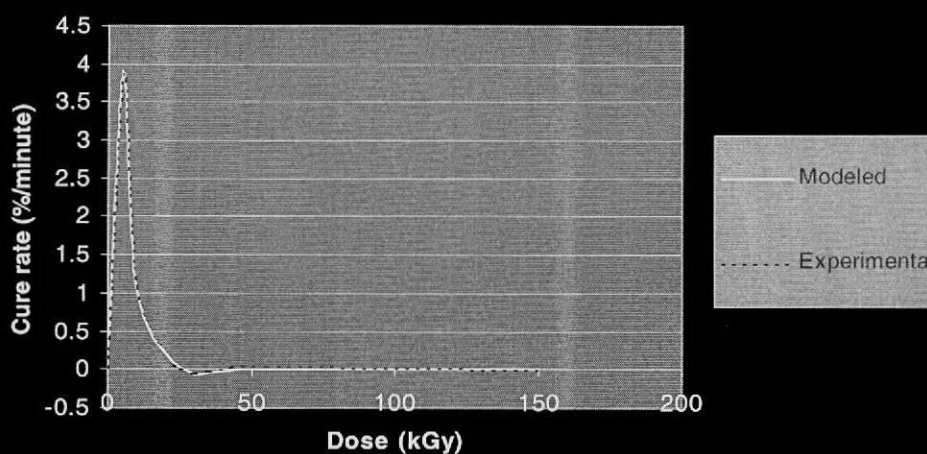
Figure 32. Experimental and modeled plots of the cure rate for the specimen with 10 phr initiator versus dose

Modeling the Heat Induced During Cure

From Equation (3), D is the heat increase due to the e-beam dose which can be directly obtained from experimental data (1 kGy = 1 kJ/kg = 1 J/g). From DSC studies of the residual exotherm for the specimen with 10 phr initiator, we get a heat liberation of 11.38 J per 1 % of cure. Therefore, the heat increase per gram due to exothermic reactions is:

$$q = degree\ of\ cure\ (\%) \times heat\ liberated\ due\ to\ 1\%\ of\ cure$$

The total heat increase per gram is the sum of D and q.

Figure 33 shows the increase in heat with increase in degree of cure. The heat increase due to exothermic reactions is proportional to the degree of cure and hence is a linear plot. The heat increase due to e-beam irradiation is much lower than the heat increase due to exothermic reactions and therefore the total heat induced in the resin is also fairly linear with respect to the degree of cure. Figure 34 shows the increase in heat with increase in dose. We can see here too, that the heat induced due to the exothermic reactions is much higher than the heat induced due to e-beam irradiation. From a degree of cure of 0.2 to 0.8 the heat induced increases approximately 4 times.

Advanced models using the finite-volume method to determine the temperature, cure kinetics and induced stress during cure have been developed by my colleague Sung-Won Moon [40].
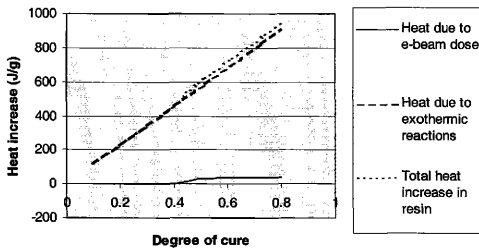
Figure 33. Total heat induced in the resin with increase in degree of cure for the specimen with 10 phr initiator
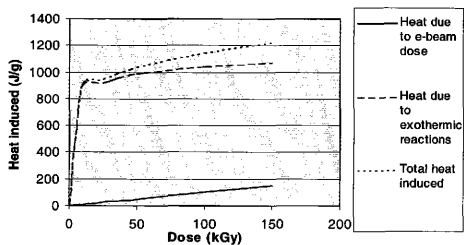
Figure 34. Total heat induced in the resin with increase in dose for the sample with 10 phr initiator concentration

Modeling the Viscosity During Cure

Equation (12) was incorporated to determine the molecular weight at different degrees of cure. The functionality of our DGEBA resin was 4 assuming perfect crosslinking. As explained earlier, there is a likelihood of reduced crosslink density due to reactions caused by water and other impurities. Therefore a value of 2.5 was chosen for the functionality. An epoxy equivalent weight (EEW) of 174 g/mole was chosen as the value of M_c. The plot relating the molecular weight to the degree of cure is shown in Figure 35.

Using suitable values for U, η_o and K from literature for a similar resin [41], in Equation (14), values of viscosity η were simulated at different degrees of cure. The temperature ranged between 30 °C and 34 °C, as measured with a thermocouple, over our required cure range and a mean value of 32 °C was chosen for calculation. The plot showing the variation of η with α is shown in Figure 36.

We now know the values of viscosity and molecular weight at the same degree of cure. These were incorporated in Equation (8) to determine the values of (s + C/RT) and (ln A + D/RT) as the slope and intercept on the ordinate axis respectively, of the mean linear plot across the points of the

$$\ln \eta \qquad \text{versus} \qquad \ln\left(\frac{MW}{MW_o}\right)$$

plot (refer to Figure 37). The value chosen for MW_o was 174 g/mole.

We can see that the molecular weight and viscosity reach a critical point between a degree of cure of 0.3 and 0.4 at which they increase sharply towards infinity. This point is the 'gel point'.

These are just simulated and not accurate values of the viscosity. Accurate experimental viscosity values can be determined from Dynamic Mechanical Analysis

(DMA) using a cone and plate type apparatus [5]. This is one of the future goals of the project.
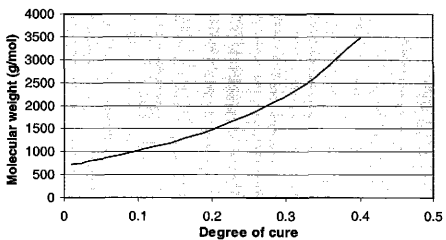
Figure 35. *Change in molecular weight with increase in degree of cure using the branching theory.*

Figure 36. Change in viscosity with increase in degree of cure

Figure 37. Determination of $(s + C/RT)$ and $(\ln A + D/RT)$ as constant values in Equation 8
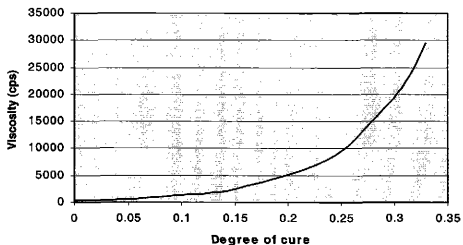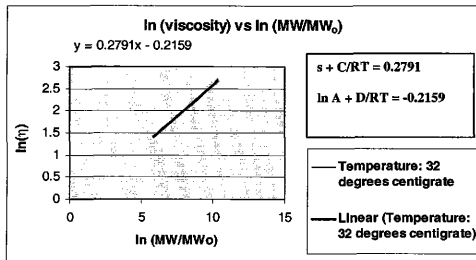
CHAPTER VI

CONCLUSIONS AND FUTURE WORK

From the experimental results, it is evident that the cure rate follows a typical arrhenius curve profile. Various authors observed this trend for thermal curing. The e-beam curing takes place well below thermal curing temperatures required to activate the catalyst. This proves the success of the method wherein the catalyst is activated by the e-beam energy without the need of increasing the temperature to above 200 $^\circ$C as in thermal curing.

The energy provided by the e-beam irradiation is much lower than the amount of energy required to cure the same material thermally and is also much lower than the energy given out due to exothermic reactions within the resin. This gives an indication that the major effect of the e-beam irradiation is to dissociate and mobilize the catalyst in a very short period of time thereby forming initiating centers uniformly throughout the specimen. Another indication of this is that most of the curing takes place at a dose of less than 10 kGy and the cure rate is much lower from a dose of 10 kGy to a dose of 150 kGy. The cure beyond a dose of 10 kGy can be considered to take place thermally due to the temperature increase. In order to accurately determine the effect of the e-beam dose rate and the initiator species and concentration, we need to conduct extensive experimental studies on the curing of the same resin – initiator system thermally as well as using e-beam irradiation with different dose rates and initiator concentrations.

A low glass transition temperature of less than 100 $^\circ$C for a conversion of 94 % as compared to a glass transition temperature of 170 $^\circ$C obtained for the same resin – initiator system when cured thermally [39] is an indication of early chain termination and fewer crosslinks. This may be caused due to the presence of moisture that cannot evaporate and escape at lower e-beam curable temperatures. Also since the curing takes place at a very high rate up to a dose of 10 kGy, the resin approaches

the gel point at an early stage of curing and the mobility of the remaining reactive chain ends and crosslinkable sites is greatly reduced.

For the experimental determination of viscosity at various doses and degrees of cure, we can use a cone and plate type Dynamic Mechanical Analysis (DMA) testing apparatus as it has been successfully done before [5]. Substituting these values of viscosity in Equation (14), we can find the activation energy for viscosity U, and the constants η_o and K. We can also calculate the constants C_1 and C_2 of Equation (13). Due to early chain termination as discussed in the previous paragraph, the molecular weight may not follow the trend of Equation (12). Experimental studies to determine the molecular weight at different doses and degrees of cure can be tried out using Gel Permeation Chromatography (GPC) and the effect of e-beam dose, initiator concentration and temperature on the molecular weight and glass transition temperature can be determined.

The highest glass transition temperature of 86 $^{\circ}$C obtained from our experiments is not adequate to meet the requirements of the future goals of the aerospace industry. However it can be improved by carefully preparing and handling the specimens to minimize contamination with moisture and other impurities. Moisture can be removed by pre heating the resin for short periods of time and by placing the sample in reduced pressure environments to bring down the boiling point of water. Also different dose rates and initiator concentrations can be tried out to reduce the speed of reactions and increase the chances of crosslinking.

Finally, the e-beam method has proved to be a successful method in curing thermosetting resins. Extensive experimental work is necessary to determine the optimum cure parameters and material component concentrations, utilizing new e-beam curable high temperature resins developed at the Polymer Technology Center at Texas A&M University with funding from the Air Force Office of Scientific Research [42].

REFERENCES

1. Goodman, S. H. (1998). *Handbook of Thermoset Plastics*. Westwood, NJ 07675: Noyes Publications.

2. Pascault, Jean-Pierre, Sautereau, H., Verdu, J. and Williams, R.J.J. (2002). *Thermosetting Polymers*. New York: Marcel Dekker, Inc.

3. Flory, P.J. (1953). *Principles of Polymer Chemistry*. Ithaca, NY 14853: Cornell University Press.

4. Prime, R.B. (1981). *Thermal Characterization of Polymeric Materials*, E.A. Turi, (eds.), Academic Press, New York.

5. Chiou, Pin-Lin (1991). Modeling the Reaction Kinetics and Chemoviscosity of an Epoxy Resin System Exhibiting Complex Curing Behavior. PhD Dissertation, Department of Mechanical Engineering, Texas A&M University.

6. Lubin, G. (1982). *Handbook of Composites*. New York: Van Nostrand Reinhold Company Inc.

7. Hoyt, A.E., Harrah, L.A., and Allred, R.E. (May 4-8, 1997). Novel Resins For E-Beam Manufacturable Composite Space Structures, *Proceedings of the 42nd International SAMPE Symposium*. 1: 509-514.

8. Cooper, W.J., Curry, R.D., and O'Shea, K.K. (1998). *Environmental Applications of Ionizing Radiation*. New York: Wiley-InterScience.

9. Russell, J.D. (1999). Air Force Research Laboratory High Temperature Composites Overview, HI TEMP Review, Paper No. 12, NASA/CP-1999-208915, Cleveland, OH.

10. Robert, R.W. (1987). *Composites, Engineered Materials Handbook Vol. 1*. Metals Park, OH 44073: ASM International, 10: 745

11. Crivello, J.V. and Lam, J.H.W (1977). Diaryliodonium Salts. A new class of Photoinitiators for Cationic Polymerization, *Macromolecules*, 10(6): 1307-1315.

12. Crivello, J.V., Lam, J.H.W., Moore and J.E., Schroeter, S.H. (1978). *Journal of Radiation Curing* 5, 2.

13. Lopata, V.J., Chung, M., Janke, C.J. and Havens, S.J. (1996). In: Electron Curing of Epoxy Resins: Initiator and Concentration Effects on Curing Dose and Rheological Properties, *Proceedings of the 28th International SAMPE Technical Conference*, Seattle, WA, 28: 901-908.

14. McGann, T.W. and Crilly, E.R. (1987). *Composites, Engineered Materials Handbook Vol. 1.* Metals Park, OH 44073: ASM International, **8**: 642

15. Clegg, D.W. and Collyer, A.A. (1991). *Irradiation Effects on Polymers.* New York: Elsevier Science Publishers Ltd.

16. Herriot, D.R. and Brewer, G.R. (1981). *Electron Beam Lithography Machines in Electron Beam Technology in Microelectronic Circuit Fabrication.* New York: Academic Press.

17. Wilson, C. G. (1983). In: Introduction of Microlithography, ACS Symposium Series 219, L.F. Thompson, C.G. Wilson and M.J. Bowden, (eds), March 20-25, Washington, D.C., pp. 87

18. Saliba, T. E. (1986). Modeling of Heat-Transfer in Advanced Composite Materials During the Cure Process, PhD. Dissertation, University of Dayton.

19. Chu, W.H. (1971). Development of a General Finite-Difference Approximation for a General Domain, Part I: Machine Transformation. *Journal of Computational Physics*, **8**: 392-408.

20. Thomson, J.F., James, F.C., and Mastin, C.W. (1974). Automatic Numerical Generation of Body-Fitted Curvilinear Coordinate System for Field containing any Number of Arbitrary Two-Dimensional Bodies. *Journal of Computational Physics*, **15**: 299-319.

21. Loos, A.C. and Springer, G.S. (1983). Calculation of Cure Process Variables During Cure of Graphite/Epoxy Composites. *Composite Materials: Quality Assurance and Processing.* ASTM STP 797: 110-118.

22. Springer, G.S. (1982). Resin Flow During the Cure of Fiber Reinforced Composites, *Journal of Composite Materials*, **16**: 400-410.

23. Servais, R.A. (1985). Private Communication, McDonnel Douglas and Lockheed Modeling Activities, May 1985.

24. Servais, R.A. Snide, J.A. and Bern, P.E. (1984). A Computer Program for Predicting Temperature Profiles Through a Laminate Stack During a Production Press-Cure Cycle, In: *SPE Annual technical Conference.* New Orleans, LA, 30 April- 3 May, pp. 736-738.

25. Gutowski, T.G., (1985), A Resin Flow/Fiber Deformation Model for Composites, *SAMPE Quarterly*, **16**(4): 58-64.

26. Soni, S.R. and Pagano, N.J. (1983). Process Models for 3-D Composites, AFWAL-TR-85-4002, Wright Patterson Air Force Base, Dayton, OH.

27. Lindt, J.T. (1982). Mechanical Principles of Formation of Fiber Reinforced Materials, *Presented at the second International Conference on Reactive Processing of Polymers*, Pittsburgh, PA.

28. Kardos, J.L., Dudukovic, M.P., McKague, E.L. and Lehman, M.W. (1983). Void Formation and Transport During Composite Laminate Processing: An Initial Model Framework. *Composite Materials: Quality Assurance and Processing.* ASTM STP 797. pp. 96-109.

29. Ma, C.M., Lee K.Y., Lee, Y.D., and Hwang, J.S. (1986). The Correlations of Processing Variables for Optimizing the Pultrusion Process. In: *Proceedings of the 31st International SAMPE Symposium.* Vol. 31. Las Vegas, NV, 7-10 April.

30. Hou, T.H. (1984). Chemoviscosity Modeling for Thermosetting Resin I, NASA Contract NASI-1600, Langley Research Center, Hampton, VA, Nov., 1984.

31. Kaetsu, I., Okubo, H., Ito, A. and Hayashi, K. (1972). Radiation-Induced Polymerization of Glass-Forming Systems. I. Effect of Temperature on the Initial Polymerization Rate, *Journal of Polymer Science*: Part. A-1, **10**: 2203-2214.

32. Flory, P.J. (1941). Molecular Size Distribution in Three Dimensional Polymers. II. Trifunctional Branching Units, *Journal of American Chemical Society*, **63**(10): 3091-3100.

33. Stockmayer, W.H. (1952),(1953). Molecular Distribution in Condensation Polymers, *Journal of Polymer Science*, **9**: 69, **11**: 424.

34. Lipshitz, S.D. and Macosko, C.W. (1976). Rheological Changes During a Urethane Network Polymerization, *Polymer Engineering and Science*, **16**(12): 803-810.

35. Macosko, C.W., and Miller, D.R. (1976). A New Derivation of Average Molecular Weights of Nonlinear Polymers, *Macromolecules*, **9**(2): 199-213.

36. Mijovic, J. (1986). Cure Kinetics of Neat Versus Reinforced Epoxies, *Journal of Applied Polymer Science*, **31**(5): 1177-1187.

37. Lee, W.I., Loos, A.C., and Springer, G.S., (1982), Heat of Reaction, Degree of Cure, and Viscosity of Hercules 3501-6 Resin, *Journal of Composite materials*, **16**: 510-520.

38. Palmese, G.R., Ghosh N.N., and McKnight, S.H., (2000). Investigations of Factors Influencing the Cationic Polymerization of Epoxy Resins. In:

Proceedings of the 45th International SAMPE Symposium, Vol 45. Long Beach, CA, 21-25 May, **45**(2): 1874-1887.

39. Defoort, B. and Drzal, T., (2001). Adhesion between Carbon Fibers and Cationic Matrices in Electron-Beam Processed Composites. In: *Proceedings of the 46th International SAMPE Symposium,* **46**(2): 2063-2074.

40. Moon, S. W., Morgan, R. J., and Lau, S. C., (2003). Hygrothermal Modeling of Thick Thermoset Resin During Electron Beam Cure – Part II: T_g-σ_y-P_v Variations and Optimization, Submitted to the *Journal of Composite Materials.*

41. Lee, W. I., Loos, A. C., and Springer, G. S., (1982). Heat of Reaction, Degree of Cure, and Viscosity of Hercules 3501-6 Resin, *Journal of Composite Materials,* **16**: 510-520.

42. Li, Y., Morgan, R. J., Tschen, F., Lu, J., Sue, H. J., Lopata, V. J., (2003). Investigation of Electron Beam Curing of Bismaleimide (BMI) and BMI/NVP Resins. In: *Proceedings of the 48th annual ANTEC Conference,* Nashville, Tennessee, 4-8 May.

VITA

Rahul Ribeiro was born in Bangalore, India in 1973. He received his B.S.in marine engineering from the Marine Engineering and Research Institute, Calcutta, India. After that, he worked for a few years in the merchant navy as a marine engineer. He came to the United States in 2000 to pursue higher studies. He graduated with an M.S. in mechanical engineering from the Texas A&M University in 2003.

His permanent address in India is:

102, Raheja Haven
12, Primrose Road
Bangalore – 560025
India.